The electromagnetic fluctuations associated with the collisional interchange instability in the equatorial-low latitude F region

E.Alam Kherani, Eurico R.de Paula, M. Mascarenhas and J.H.A. Sobral INPE SJC, Brazil

This paper was prepared for presentation at the 11th International Congress of the Brazilian Geophysical Society, held in Salvador, Brazil, August 24-28 2009.

Abstract

The excitation of electromagnetic fluctuations by the collisional interchange instability (CII) in the equatorial-low-latitude ionosphere is studied. The hydromagnetic equations are used to obtain the governing equations for the density, electric field, currents and magnetic field fluctuations in the ionosphere. These equations are linearized and solved in the three-dimensional environment around equator, taking into account both parallel and perpendicular (to Earth's magnetic field) dynamics of ionosphere. The excitation of CII in the equatorial-low-latitude Ionosphere, the nature of associated electromagnetic and current fluctuations, the mapping of equatorial polarization electric field to the off-equatorial latitudes are the aspects pursued in the present study. In addition, the possible effects of trans-equatorial wind in the growth of CII, which is recently being reported from COPEX observations over Brazil, are also studied.

Introduction

The equatorial F region of terrstrial ionosphere often reveals the presence of irregularities during evening time. These irregularities occupy wide altitude range, have wide spectrum ranging from km to meter scales and this phenomena is termed as Equatorial spread F (ESF) [*Balsley et al, 1971*]. In the initial stage of the ESF, the positive density gradient in the bottomside of F region becomes unstable under the action of Collisional-Interchange instability (CII) mechanism and gives rise to the rapidly moving upwelling depletions or bubbles [*Haerendel, 1973*; *Sultan, 1996*].
The coordinated equator-low-latitude observations has revealed several interesting aspects of bubble dynamics surrounding the equator [*Tsunoda, 1979*; *Abdu et al, 1992*; *Sobral et al, 1990*]. It has been found that the bubble is developed first at the equator and then grows and maps to other latitudes. These observations have also shown that the bubble growth is influenced by the off-equatorial dynamics and vise versa [*Tsunoda, 1979*; *Abdu et al, 1992*; *Sobral et al, 1990*]. The 2D field-align-integrated (FAI) models are developed to understand the bubble dynamics at and around the equator [*Sultan, 1996*; *Rapaport, 2001*]. These studies have shown that the growth of the CII is fastest at the equator owing to the pre-reversal enhancement electric field and large density gradient present there [*Sultan,* 1996]. This approach has also shown the importance of off-equator dynamics to controle the growth of CII. It is found that due to the large conductivity parallel to the terrestrial magnetic field, the growth of CII at the equator is is affected by the off-equator dynamics and vise versa [*Sultan,* 1996]. More recently, *Alam et al* [2005] have derived the explicit 3D growth rate of CII at and around the equator. It is found that the coupling between equator and off-equator enters through Pederson conductivity and field-aligned currents (FACs). They have also shown that once the local 3D growth rate is projected at equator by integrating over off-equator latitude, it becomes equivalent to the FAI growth rate.
All these analyses assume electrostatic condition for the growth of CII. Under this condition, the parallel (to the terrestrial magnetic field) polarization electric field and fluctuating wave-vector are ignored. Noting that the radar observations have indeed found the high aspect sensitivity associated with the ESF and bubble, the electrostatic condition seems to be the prevailing condition during the excitation of CII.
Bhattacharya and Burke [2001] and *Basu* [2004] have relaxed the electrostatics condition and studied the electromagnetic fluctuations associated with the CII. *Bhattacharyya and Burke* [2000] have invoked the finite parallel wavenumber associated with the Alfven waves. Under such condition, large FACs is expected to flow which is supported by the perpendicular (to the terrestrial magnetic field) magnetic fluctuation associated with Alfven Waves. The bottomside F region is connected to low Pederson conductivity underlying region through FACs and Alfven waves. The presence of FACs causes the reduction in the polarization current responsible for the polarization field of CII. Since this field grows with time, more and more polarization currents are taken away by the Alfven wave. It is thus important for the growth of CII that the Alfven Wave damps as it propagates away from the equator. *Basu* [2004] has also discussed the non-local growth of CII relaxing the electrostatic condition. He has found that the perturbed toroidal magnetic field which arises due to the FACs, dissipates away due to the large parallel conductivity and consequently its amplitude remains small. This indicates that the CII mode in the equatorial ionosphere is predominantly electrostatic.
An interesting aspect of magnetic signatures associated with the CII is recently being brought from the CHAMP satellite observation [*Stolle et al,* 2005]. They have observed the magnetic signatures associated with the depletion which is mapped to the equatorial ionization anomaly (EIA) region. The amplitude of magnetic fluctuations is found to be in the range of nT and anti-correlation is noted between the observed fluctuation in

the northern and southern EIA regions. The anticorrelation indicates the existence of oppsite propagating Alfven waves excited by the FACs inside the depleted flux tube. This is in confirmation with the electrodynamical model of bubble discussed by *Bhattacharya and Burke* [2001]. They have also suggested that the pressure driven perpendicular current may excite the parallel magnetic fluctuations. In other words, the current perpendicular to the magnetic field is the principle source of magnetic fluctuations.
These studies suggest that the nature of current flow in and around the bubble is one of the important aspect which needs more attention to understand the expected magnetic field fluctuations. The present work is an effort to develop a linear electromagnetic model of CII in the three-dimension geometry around the equator. It deals with the topics such as the the growth of CII under electromagnetic condition, the nature of current system associated with the growth of CII, corresponding electromagnetic fluctuations amplitudes. In addition, the effect of trans-equatorial wind (TEWs) in the growth of CII is also studied. We carry out the linear analysis of CII in the frame work of hydromagnetic theory. In section 2, the formalism is presented where the closed set of linearized equations for density, polarization electric field, current and magnetic fields are derived. The detailed steps of derivations are described in Appendix A. In section 3, the results concerning the different aspects of the growth of CII and related electromagnetic and current fluctuations are discussed.

Simulation model

In the hydromagnetic framework, we adopt following set of equations in dipole coordinate system:

$$0 = -c_s^2 \nabla \log n_s + \frac{q_s}{m_s}(\vec{E} + \vec{u}_s \times \vec{B}_o) - \nu_s \vec{u}_s + \nu_s \vec{W} + \vec{g} \quad (1)$$

$$\frac{\partial n_s}{\partial t} + \nabla.(n_s \vec{u}_s) = 0 \quad (2)$$

$$\vec{J}^W = e(n_i \vec{u}_i - n_e \vec{u}_e) \quad (3)$$

The governing equations for fluctuating electric field $\delta\vec{E}$ is given by following equations:

$$\frac{\partial \delta E_p}{\partial t} - \gamma_p' \delta E_p - \gamma_p \delta E_\phi + \eta \Delta U_p^o \left(\frac{\partial \delta E_q}{h_q \partial q} + \frac{\delta E_q}{l_q} \right) = s_p \quad (4)$$

$$\frac{\partial \delta E_\phi}{\partial t} - \gamma_\phi' \delta E_p - \left(\gamma_\phi + \frac{U_q}{l_q} \right) \delta E_\phi + \eta \Delta U_\phi^o \left(\frac{\partial \delta E_q}{h_q \partial q} + \frac{\delta E_q}{l_q} \right) = s_\phi \quad (5)$$

$$\frac{\partial \delta E_q}{\partial t} - \gamma_q' \delta E_p - \gamma_q \delta E_\phi + \frac{m_e}{m_i} \Delta U_q^o \left(\frac{\partial \delta E_q}{h_q \partial q} + \frac{\delta E_q}{l_q} \right) - D_\parallel \nabla^2 \delta E_q = s_q \quad (6)$$

The current and magnetic field fluctuations $(\delta\vec{J},\ \delta\vec{B})$ are obtained by solving Ohm's law and wave equation for the magnetic field:

$$\delta\vec{J} = \hat{\sigma}.\delta\vec{E} + \vec{J}^W \quad (7)$$

$$\nabla^2 \delta\vec{B} - \frac{1}{c^2}\frac{\partial^2 \delta\vec{B}}{\partial t^2} = -\mu_o \nabla \times \delta\vec{J} \quad (8)$$

$$\gamma_p = -\frac{e n_o \rho_H \Delta U_{op}}{\sigma_P l_p}; \quad \gamma_\phi = -\frac{e n_o \rho_H \Delta U_{o\phi}}{\sigma_P l_p}; \quad \gamma_q = -\frac{e n_o \rho_H \Delta U_{oq}}{\sigma_\parallel l_p}$$

$$\gamma_p' = \frac{e n_o \rho_P \Delta U_{op}}{\sigma_P l_p}; \quad \gamma_\phi' = \frac{e n_o \rho_P \Delta U_{o\phi}}{\sigma_P l_p}; \quad \gamma_q' = \frac{e n_o \rho_P \Delta U_{oq}}{\sigma_\parallel l_p}$$

$$\eta = \frac{m_e \sigma_\parallel}{m_i \sigma_P}, \quad D_\parallel = \frac{1}{\mu_o \sigma_\parallel}$$

where $(n_s,\ \vec{u}_s)$ are the number density, velocity of plasma fluid 's' $(\mathrm{s = ions(i)/electrons(e)})$, $(q_{i,e} = \pm e)$, $(\vec{W},\ \vec{g})$ are the amplitudes of wind and gravitational acceleration respectively, ν_s is the frequency of collision between species s-to neutral, $\vec{B}_o$ is the Earth's magnetic field and $\vec{J}^W$ is the ionospheric current density caused by mechanical forces such as the wind and pressure gradient. $(\vec{E},\ \vec{J},\ \vec{B})$ in above equations are the fluctuating electric field, net current and magnetic field in the ionosphere, $\underline{\sigma}$ is the ionospheric conductivity tensor and $(c_s = \sqrt{\frac{kT_s}{m_s}},\ c = \frac{1}{\sqrt{\mu_o \varepsilon_o}})$ are the thermal velocity of species 's' and the speed of light respectively. Here $(T_s,\ m_s)$ are the temperature and mass of the ionospheric species 's' and $(\mu_o,\ \varepsilon_o)$ are the magnetic susceptibility and dielectric permittivity in the vaccum. We assume temperature of ions and electrons to be the same as the temperature of neutral particles in the atmosphere. Also, we neglect the production and loss of ions and electrons by photoionization and chemcal reactions in (2).

Results and Discussion

Equations (1-8) form the closed set of equations to determin the density and electromagnetic fluctuations excited by CII. They are the coupled-non-linear equations and should be solved numerically. However, in present study, our focus is rather on the (a) linear growth characteristics of CII without electrostatic condition, (b) the study of current system driven by CII and shear Alfven wave and (c) the growth of magnetic fluctuations. Moreover, we shall also be dealing with the growth of CII influenced by parallel dynamics mainly the effects of trans-equatorial wind.
In Figure 1a, the initial density n_o is plotted. The superimposed vectors represent the dipole magnetic field of Earth. The equatorial density profile and collision frequencies are chosen to be same as chosen in the earlier study [*Alam et al,* 2004]. In the growth terms $\gamma' s$ and the source term $\vec{s}$ in (4-6), the ambient forces such as the pressure, wind, gravity and electric fields appear. At first step, to understand the growth characteristics of electromagnetic and current fluctuations by CII, all the forces except gravity and $E_{\phi o}$ are assumed to be zero. These two are the principle forces known to be responsible for the growth of CII in the F region [*Haerendel*, 1973]. The $E_{\phi o}$ is assumed to be homogeneous-uniform with 1 mV/m magnitude and in the eastward direction. With these inputs, different growth terms appearing in (A9-A11) are estimated. In Figure 1b, the meridional distribution of growth rate of CII γ_ϕ is plotted.

Linear growth of electromagnetic fluctuations

In Figure 2, the time evolution of maximum values of $\delta E_{p,\phi,q}$ are plotted. It can be seen that the components $\delta E_{p,\phi}$ grow exponentially indicating the linear growth of CII. The growth of δE_q is different from them and does not show any tendency of exponential growth. It should be pointed out that there is an indication of positive growth of δE_q inspite that the diffusion rate is faster than the growth rates in (15). This is because of very large amplitude of δE_ϕ which appears with growth rates in (15). The largest component is the δE_ϕ ($\sim$ 0.2 mV/m) which is the principle polarization field of CII.

In Figure 3a-c, the distribution of $\delta E_{p,\phi,q}$ at $t_g = \gamma_\phi t =$ 0.8 are plotted in the meridional plane. We note that the meridional distribution of δE_ϕ in the linear phase follows the trend of γ shown in Figure 1b which is expected. The component δE_p also grows similar to the δE_ϕ and its meridional distribution is also similar to the growth rate distribution shown in Figure 1b. In contrary, the growth and distribution of δE_q is entirely different. While $\delta E_{p,\phi}$ tends to be maximum near the equator, δE_q tends to be maximum at the higher latitude close to the upper boundary of E region. It can be seen that along any field line at F region apex height, $\delta E_{p,\phi}$ decrease with increasing dip-angle and become negligible at the end of field line. In contrary, δE_q has tendency to increase along the field beyond certain dip-angle and become maximum at the end of field lines. These kind of variations of $\delta E_{\phi,q}$ are consistent with the variations noted by *Basu* [2004] in his Fourier-transformed nonlocal approach. He has found that the δE_q becomes maximum near the end of field line where parallel conductivity is small. On the other hand, δE_ϕ remains large at the beginning of field line where Pederson conductivity is large. Near the end of field line, the Pederson conductivity is small and is not able to sustain δE_ϕ and as a result, it becomes negligible in this region.
In Figure 3d-f, δj distributions for estimated δE are shown at $\gamma_\phi t = 0.8$. We note that the δj_ϕ is the principle component and maximizes at the equator. The component δj_p is the smallest component while FAC, δj_q, is of intermediate magnitude. The magnetic field fluctuations shown in Figure 3g-i follows the current distribution. It is noted that the the largest fluctuation in the F region is the δB_ϕ but at the off-equator latitude. At the equator, it is either of components $\delta B_{p,q}$ which maximizes in the F region due to the large FACs and δj_ϕ.
The results presented in this section can be listed as follows: (1) $\delta E_{\phi,p}$ grows exponential during the linear phase of CII while the growth of δE_q is strongly influenced by parallel diffusion, (2) Along any field line with apex height in the F region, $\delta E_{\phi,p}$ are maximum near the beginning of field line. On the other hand, δE_q becomes maximum near the beginning or end of field line depending on the apex height of field line, (3) $\delta E_\phi, \delta j_\phi, \delta B_{phi}$ are the dominant components of fluctuations excited in the F region, (4) The fluctuations δB_ϕ however maximizes at the off-equator latitude, (5) Near the equator, it is either of $\delta B_{p,q}$ which maximizes in the F region.

The effects of transequatorial wind (TEW)

The recent COPEX campaign from the Brazil founds the decrease in the spread F activity in the presence of TEWs [*Abdu et al, 2008*]. Similar kind of effects had been noted from earlier observations [*Mendillo et al,* 1998]. Recently, *Alam et al* [2004] have derived the expression for the growth rate which explicitly includes the effects of TEWs. It was argued that effect of TEWs is to drive a current which act against the growth of CII. No quantitative analysis was presented though. In present study, this aspect can be studied quantitatively by including the U_q/l_q term in equation (5) which is neglected so far. To do so, the uniform $U_q = 50$ m/s at all altitudes are chosen. The density scale height along field line, l_q, is obtained self-consistently by including the effect of TEWs in the continuity equation (2) also. In Figure 4, the growth of δE_ϕ is plotted with and without U_q/l_q term in the (5). It is noted that the growth of δE_ϕ is reduced in the presence of U_q/l_q term. This is an indication of the damping effect of TEWs in the growth of CII. It is also noted that δE_q grows faster with TEWs than without TEWs. This is again an indication of reduction in the growth of CII since large δE_q drives large FACs which in turn reduces the growth of CII [*Bhattacharya and Burke*, 2000].

Summary and Conclusions

We here study the 3D linear growth of collisional interchange instability (CII) without electrostatic condition in the equatorial-low-latitude ionosphere. To do so, the hydromagnetic equations are used to derive the governing equations for the collisional-interchange instability. The governing equation of polarization field $\delta\vec{E}$ includes the growth, diffusion, mapping and source terms. The growth of perpendicular polarization fields are mainly determined by the CII growth. The parallel component is strongly influenced by the large diffusion determined by the parallel conductivity. Still, it has weak tendency to grow depending on the magnitude of perpendicular component. The perpendicular component associated with CII does not diffuse provided the damped shear Alfven wave propagates along the Earth's field line. The phase velocity of this wave is determined by the Pederson conductivity and it damps with the rate equal to the CII growth rate. Without this wave, the CII is strongly damped by the diffusion. Along any field line, the perpendicular component maximizes at the beginning of field line. On the other hand, the parallel component maximizes either at the beginning or end of field line depending on the apex height of field lines. The dominant components of electromagnetic fluctuations are the δE_ϕ, δj_ϕ at all latitudes and δB_p near the equator. At the off-equator latitude, δB_ϕ is found to be the dominant component. The effects of trans-equatorial wind on the growth of CII are also studied. It is found that the growth of CII reduces in the presence of trans-equatorial wind which confirms the recent COPEX observations from the Brazil.

References

Abdu et al, An overview of COPEX observations over Brazil, *submitted to J. Geophys. Res.*, 2008
Abdu, M. A., I. S. Batista, J. H. A. Sobral, A New Aspect Of Magnetic Declination Control On Equatorial Spread-F And F-Region Dynamo, J. Geophys. Res., 97(10), 14897, 1992.
Balsley, B.B., G. Haerendel and R.A. Greenwald, Equatorial spread F: Recent observations and a new interpretation, J. Geophys. Res., 77, 5625, 1972.
Basu B., On the linear theory of equatorial plasma instability: Comparison of different descriptions, J.

Geophys. Res. 107, 10.1029/2001JA000317, 2002.
Basu B., Characteristics of electromagnetic Rayleigh-Taylor modes in the nighttime equatorial plasma, JGR 110, 10.1029/2004JA010659.
Bhattacharya A. and Burke W.J., A transmission line analogy for the development of equatorial plasma bubble, JGR 105, 24, 941, 2000.
Haerendel, G., Theory of equatorial spread F, Preprint, Max-Plank Institute fur Extraterr. Phys., 1973.
Kelley M.C., J.J. Makela, B. Ledvina and P.M. Kintner, Observations of equatorial spread F from Halekala, Hawaii, J. Geophys. Res., 29 (20), doi:10.1029/2002GL015509, 2002.
E. Alam Kherani, M. Mascarenhas, J.H.A. Sobral, E.R. de Paula and F.C. Bertoni, A three dimension simulation model of collisional interchange instability, Space Science Review, 121, 253-269, (2005).
Rappaport H.L. (1998), Localized modes with zonal neutral wind, diffusion, and shear in equatorial spread F, JGR 103, A12 29137-29154.
Sobral, J. H. A., and Abdu, M. A. "Latitudinal Gradient In The Plasma Bubble Zonal Velocities As Observed By Scanning 630mm Airglow Measurements", J. Geophys. Res., 95(A6), 8253, 1990.
Stolle C., H. Luhr, M. Rother and G. Balais, Magnetic signatures of eaquatorial spread F as observed by the CHAMP satellite, JGR 111, 10.1029/2005JA011184, 2006.
Sultan P.J, Linear theory and modelling of the Rayleigh-Taylor instability leading to the occurrence of equatorial spread F, J. Geophys. Res., 101, 26675, 1996.
Tsunoda R. T., M.J. Baron, J. Owen and D.M. Tole, ALTAIR: An incoherent scatter radar for equatorial spread F, Radio Sci., 14, 1111, 1979.

Acknowledgments

EAK thanks FAPESP for the grant under process number 2007/00104-0 and INPE for providing research facility.

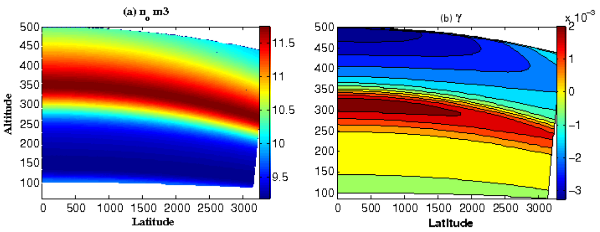

Figure 1: (a)The Altitude-Latitude distribution of density n_o and (b) growth rate distribution.

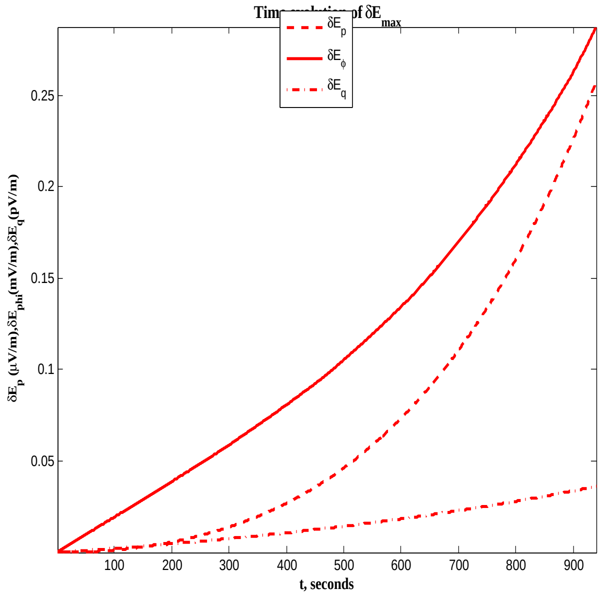

Figure 2: The time evolution of three component of δE_{max}.

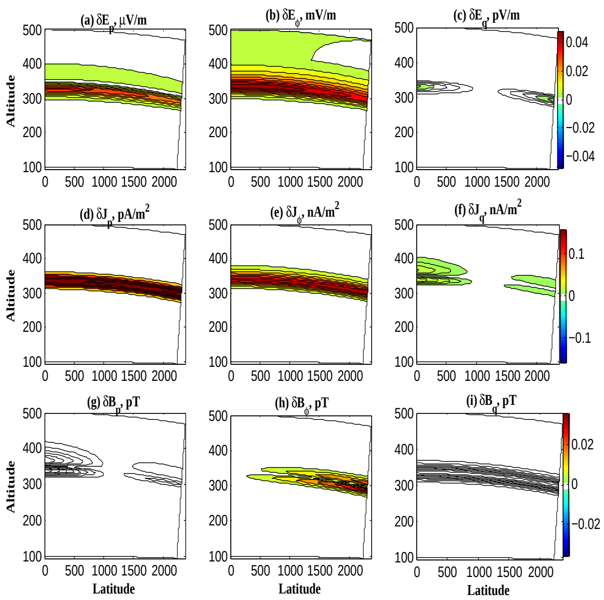

Figure 3: The distribution of three component of (a) δE, (b)δj and (c)δB at $\gamma t = 0.8$

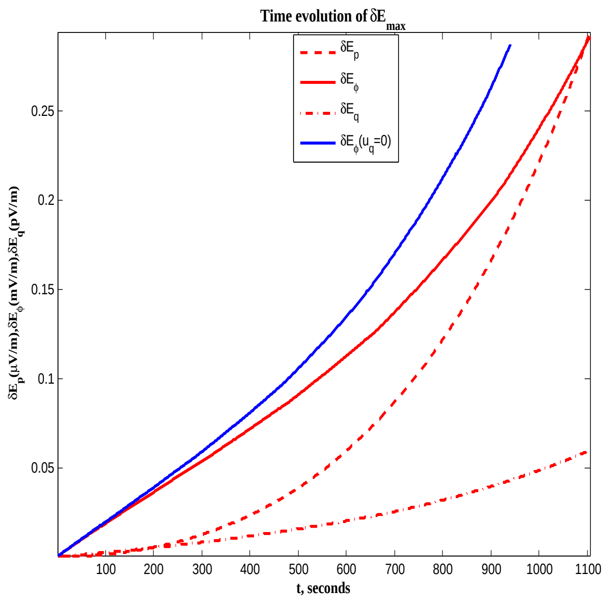

Figure 4: The time evolution of three components of δE_{max} with trans-equatorial wind. The time evolution of δE_{ϕ} without trans-equatorial wind is also plotted for the comparision.